Range-resolved optical detection of honeybees by use of wing-beat modulation of scattered light for locating land mines

David S. Hoffman, Amin R. Nehrir, Kevin S. Repasky, Joseph A. Shaw, and John L. Carlsten

An imaging lidar instrument with the capability of measuring the frequency response of a backscattered return signal up to 3.6 kHz is demonstrated. The instrument uses a commercial microchip frequency-doubled pulsed Nd:YAG laser with a 7.2 kHz pulse repetition rate, a pulse duration of less than 1 ns, and a pulse energy of greater than 10 μJ. A 15.2 cm commercial telescope is used to collect the backscattered signal, and a photomultiplier tube is used to monitor the scattered light. This instrument is designed for range- and angle-resolved optical detection of honeybees for explosives and land-mine detection. The instrument is capable of distinguishing between the scattered light from honeybees and other sources through the frequency content of the return signal caused by the wing-beat modulation of the backscattered light. Detection of honeybees near a bee hive and spatial mapping of honeybee densities near feeders are demonstrated. © 2007 Optical Society of America

OCIS codes: 280.0280, 280.3420, 120.0280, 120.4640.

1. Introduction

An estimated 50×10^6 unexploded ordnances (UXOs) are scattered through roughly 90 countries killing approximately 15,000–20,000 people each year.[1] Current detection methods for UXOs include sweeping hand-held metal detectors over suspected minefields.[1] This method, however, puts the operator at risk and results in large false-alarm rates resulting from the inability to differentiate between UXOs and other metallic objects. The hand-held metal detector is also unable to detect the plastic and plasticlike materials used in some UXOs resulting in missed targets.

Active research in UXO detection includes electromagnetic induction, infrared and hyperspectral imaging, electrical impedance tomography, ground penetrating radar, electrochemical methods, and biological methods.[1] Perhaps the most widely known biological method of UXO detection is the use of dogs. Dogs possess the ability to detect small concentrations of vapor from UXOs. Phelan *et al.*[2] determined that the chemical vapor sensitivity of dogs for 2.4 dinitrotoulene (2.4-DNT) is of the order of 10^{-18} g/ml. However, dogs require working with a handler in a minefield, putting both the dog and handler at risk.

A second biological method for land-mine detection currently under investigation is the use of honeybees to detect the chemical vapors associated with UXOs.[3–6] Bromenshenk *et al.*[5] showed that properly conditioned honeybees can detect 2.4-DNT at vapor densities below 50 parts per 10^{12} with a probability of less than 2% of either a false positive or a false negative. Using a simple operant conditioning technique, an entire colony of local honeybees can be trained in 2 days to actively seek vapor plumes from UXOs using their sense of smell and natural foraging behavior.

The demonstrated ability of honeybees to detect UXOs has led to a need to remotely detect the presence and dwell time of honeybees in flight. Optical sensing techniques are one method of detection currently under investigation. In 2002, researchers at Sandia National Laboratory demonstrated the ability of a direct-detection lidar instrument for honeybee detection.[7] The direct-detection lidar works by sending out a pulse of light into a desired honeybee detection area and detecting backscattered light as a function of range. Light scattered from bees that were

All authors except J. Carlsten are with Electrical and Computer Engineering, Cobleigh Hall Room 610, Montana State University, Bozeman, Montana 59717, USA. K. S. Repasky's e-mail address is repasky@ece.montana.edu. J. Carlsten is with the Department of Physics, EPS 264, Montana State University, Bozeman, Montana 59717, USA.

Received 20 November 2006; accepted 9 January 2007; posted 22 January 2007 (Doc. ID 77176); published 1 May 2007.

0003-6935/07/153007-06$15.00/0

© 2007 Optical Society of America

located near a beehive placed 1 km away from the lidar instrument was collected and used to determine the presence of honeybees within the field of view of the lidar instrument. Ranging information was determined by the time of flight of the light. In 2003, an experiment was performed at Fort Leonard Wood, Missouri that demonstrated the ability of honeybees to detect plumes from UXOs and the ability of a direct-detection scanning lidar to locate the bees.[8] In this experiment, honeybees were conditioned to find UXOs and released over a 24 m wide by 44 m long field containing buried UXOs. The honeybees were detected using a scanning direct-detection lidar instrument. By keeping track of the angle of the instrument relative to the field, a map of the honeybee density was generated. A higher bee density was found that corresponded to the location of the UXO vapor plume demonstrating the ability of mapping out UXOs using conditioned honeybees. However, Shaw *et al.* noted that the direct-detection lidar could not distinguish the signal from light scattered from a honeybee and light scattered from other sources such as vegetation, and noted the need for a bee-specific detection method.[8]

One possibility for a bee-specific detection method is to use the modulated light scattered from the wings of a honeybee.[9–12] The modulated light scattered from the wing of a honeybee will have a characteristic frequency of 200–300 Hz and can be used to distinguish the light scattered from a honeybee from the light scattered from stationary or near-stationary vegetation. Repasky *et al.*[12] demonstrated an optical detection technique based on wing-beat modulation of the scattered light using a continuous-wave laser source that was able to distinguish between honeybees and other objects in a cluttered environment. However, because the instrument used a continuous-wave laser source, range information could not be determined through the time of flight of the laser pulses making this instrument unsuitable for spatially mapping honeybee densities.

In this paper, we present a direct-detection lidar instrument that uses a pulsed laser source that can be used for mapping honeybee spatial densities. The pulsed laser has a pulse repetition frequency (PRF) greater than the Nyquist frequency[13] associated with the modulated signal due to the scattered light from the moving wings of a honeybee and thus can be used to provide range-resolved bee-specific detection in the following manner. A laser pulse is sent out and the return signal as a function of range is recorded. A second laser pulse is sent out at a time 1/PRF later than the first pulse, and the return signal as a function of range is recorded. This is repeated until a data matrix is formed with each element of the data matrix corresponding to the return signal from a particular range at a particular time. Thus, the return signal as a function of time from a particular range is now recorded as a discrete time signal with a time interval of 1/PRF. Now, the modulated wing-beat signal can be sought at a particular range thus yielding range-resolved bee-specific detection.

This paper is organized as follows: The pulsed direct-detection lidar instrument is described in Section 2. Experimental results are presented in Section 3, including an experimental demonstration of mapping bee densities using the pulsed lidar instrument. Finally, some brief concluding remarks are presented in Section 4.

2. Experimental Setup

A. Hardware

A schematic of the pulsed direct-detection lidar instrument for range-resolved detection of honeybees using the wing-beat modulated scattered light is shown in Fig. 1. A frequency-doubled Nd:YAG microchip laser (JDSU NG-10320-100) is used as the laser source for the lidar instrument. The laser operates at a wavelength of 532 nm with a pulse duration of less than 1 ns, a pulse repetition frequency of 7.2 kHz, and a pulse energy of greater than 10 μJ. The output of the laser is reflected by a steering mirror onto a second dielectric mirror. A small part of the beam passes through the dielectric mirror and is incident on a fast photodetector (New Focus model 1621) used as a trigger detector. The light reflected from the dielectric mirror is next sent through two lenses used to expand and collimate the beam. The collimated light is then incident on a 20.3 cm by 40.6 cm front surface aluminum scanning mirror used to direct the beam into the field. The mirror is mounted on a computer-controlled rotational mount (Zaber Technologies) that utilizes a high-resolution stepper motor. The manufacturer stated resolution of the rotational mount is less than 2 μrad. Light scattered from objects in the field is reflected from the scanning mirror into a 15.2 cm diam Maksutov telescope. The lidar instrument is set up in a bistatic configuration so that overlap is achieved due to a small angle of the transmitted beam relative to the field of view of the telescope. After the telescope, the light is further focused and passes through two narrowband interference filters. Each filter has a center wavelength of 532 nm with a 3 nm full width at half-maximum bandwidth. Finally, the light is detected using a photomultiplier tube that provides a voltage

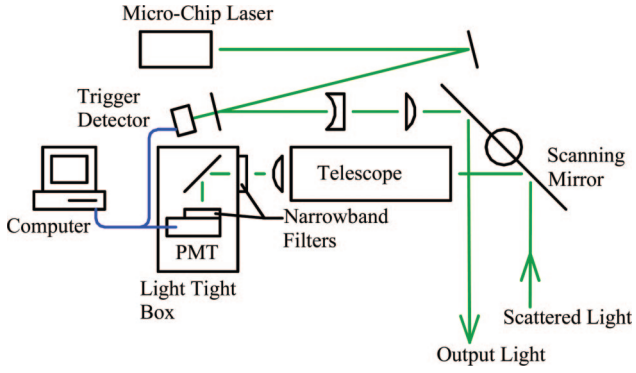

Fig. 1. (Color online) Schematic of the imaging lidar instrument for honeybee detection.

signal that is proportional to the amount of transmitted light scattered back to the receiver. A high-speed analog-to-digital (A/D) card (Gage Electronics) is used to record the signal from the voltage generated from the photomultiplier tube (PMT). This 12 bit A/D sample rate is 200 MHz, setting the range resolution of the instrument at 0.75 m.

B. Software

The software for controlling the scanning mirror and acquiring data via the A/D card was written using LABVIEW. During the operation of the laser system, the return light from each outgoing laser pulse is sampled at 200 MHz with the 12 bit A/D card. The data are stored in a matrix in the following manner. The first laser pulse is detected by the trigger detector starting the acquisition of the PMT voltage as a function of time. The range can be related to time through the time of flight of the laser pulse to the scatterer plus the time of flight of the scattered light back to the receiver. Because the A/D card can sample at 200 MHz, a PMT voltage is read and stored every 5 ns setting the range resolution limit of the direct detection lidar at 0.75 m, which corresponds to one range bin. The PMT voltage can be read for a set time (or range) that is set in the acquisition program and these data are stored as the first column in the data file. The second laser pulse occurs at a time 140 μs after the first pulse. Again, the second laser pulse is seen by the trigger detector and starts the data acquisition of the PMT voltage as a function of range and is written as a second column in the data file. This process is repeated for a user-defined number of laser pulses until a two-dimensional array is created as shown schematically in Fig. 2. This array is saved as a data file for future analysis. A discrete time signal at a particular range can be assembled now by looking at the return signal from successive laser pulses at a particular range bin. This will produce a discrete time signal with a 140 μs interval between data points resulting in a Nyquist frequency of 7.2 kHz.[13] The maximum frequency that can be detected using the discrete time signal is thus 3.6 kHz, well above the 300 Hz signal expected from the modulated return signal due to the wing-beat motion of the honeybees.[13] The scanning mirror is stepped to a new position, and the above process is repeated. In this manner, both range- and angle-resolved data can be generated and used to create a two-dimensional map of honeybee density.

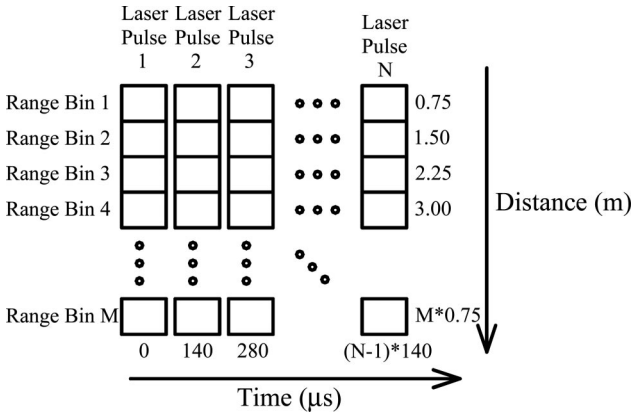

Fig. 2. Schematic of the two-dimensional array used to store and process the data taken by the instrument shown in Fig. 1.

Software for interpreting the saved lidar data was developed using MATLAB. First, each two-dimensional array of data is broken into ten time windows. This is done to help detect honeybees, which may only be within the transmitted laser beam for part of the time over which data are being collected. Each time window is then analyzed to determine if a significant amount of light was scattered back to the receiver during that time. The threshold light level is calculated for each range as a percentage of the median light return from that range. The percentage of the median light used for the threshold is experimentally determined at the beginning of each field test when initial scans are taken to allow for varying lighting conditions. In this way, the threshold condition is different for each range bin, but relies only on one input parameter. Only those time windows where a significant amount of backscattered light was detected are passed on for further analysis. This analysis is done first to speed up the data processing. A fast Fourier transform (FFT) of these remaining windows is conducted for each range bin in which backscattered light was detected resulting in a series of frequency spectra as a function of range. These spectra are then analyzed to determine if they contain peaks in the 200–300 Hz frequency range associated with the wing beats of honeybees. This analysis consists of comparing the median of the spectrum within the wing-beat frequency range to the median of the entire spectrum. Before this comparison is carried out, most of the low-frequency noise is cut out of the spectrum to reduce the effects of large low-frequency spikes on the outcome of the comparison. This removal of the lowest parts of the frequency spectrum is carried out digitally after the data have been transformed into the frequency domain. This process is repeated for the data from each angle of the stepper motor, resulting in a map of honeybee counts as a function of range and angle. When data have been collected over the same set of angles multiple times, the honeybee counts from all of these passes are added together, yielding a honeybee density map.

3. Bee Detection

Initial testing of the detection of honeybees with the instrument described in the previous section was carried out at an outdoor beehive. The instrument was scanned near the beehive to ensure that honeybees would fly through the laser beam. A plot of the voltage signal is shown in Fig. 3 with range plotted on the vertical axis and time plotted on the horizontal axis. The false-color image represents the strength of the signal detected by the PMT. In this figure, the modulated signal from a honeybee can be seen at the range of 23 m, while background vegetation produces an unmodulated signal starting at the range of 33 m.

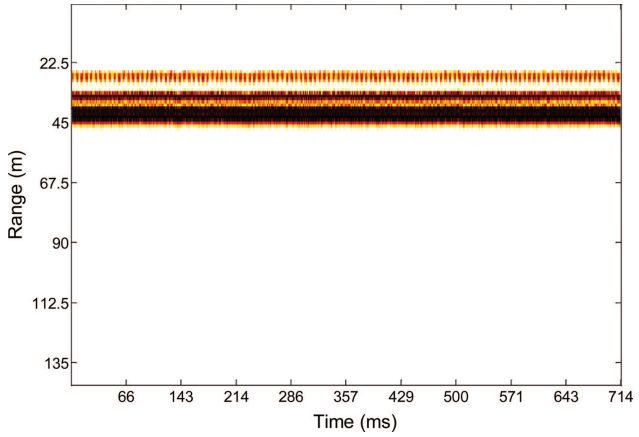

Fig. 3. (Color online) False-color image represents the strength of the return signal from a particular range as a function of time. In this figure, a modulated return signal is seen at a range of 23 m, while an unmodulated signal is seen at a range of 33 m. The modulated signal is due to a honeybee, while the unmodulated signal is due to vegetation.

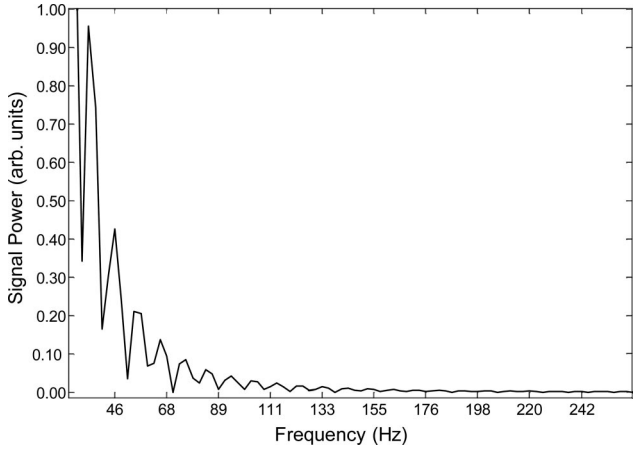

Fig. 5. Plot of the signal power as a function of frequency is shown for the return signal at a range of 33 m shown in Fig. 3. This plot was generated using a discrete Fourier transform that shows an unmodulated return signal indicating that light was scattered from a stationary object. In this case, the scattering object was observed to be vegetation.

A plot of the FFT of the discrete-time signal from the 23 m range is shown in Fig. 4. In this figure, the FFT shows a peak at 220 Hz that is associated with the light scattered from the wing-beat motion of the honeybee. A plot of the FFT of the discrete time signal from the 33 m range is shown in Fig. 5. No signal is seen in the 200–300 Hz frequency window indicating that light was scattered from a stationary source. These two figures indicate the instrument's ability to discriminate signals according to their frequency content.

A second plot of the voltage signal is shown in Fig. 6 with range plotted on the vertical axis and time plotted on the horizontal axis; the false-color image represents the strength of the signal detected by the PMT. In this plot, the background vegetation again produced a strong return signal at 35 m. Three signals are seen at 23, 25, and 30 m at approximately 70, 340, and 640 ms, respectively. A plot of the FFT of the discrete time signal from a range of 25 m is shown in Fig. 7. The FFT shows a peak at 220 Hz indicating the return signal from 25 m is due to the scattered light from the wing-beat motion of the honeybee. Similar results are seen for FFTs of the discrete time signals from ranges of 23 and 30 m. A plot of the FFT for the return signal at a range of 36 m, where a strong return signal is seen from background vegetation, is shown in Fig. 8. Here, there is no indication that the scattered light is modulated at frequencies associated with the wing-beat motion of honeybees. Data in Figs. 3 and 6 can also be used to determine honeybee dwell times. For example, in Fig. 3, the honeybee is hovering in the beam for over 700 ms, while in Fig. 6, the honeybees are in the laser beam for less than 50 ms. Dwell time may be useful infor-

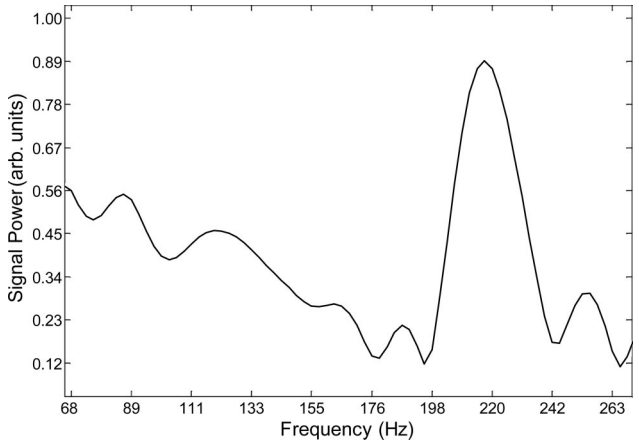

Fig. 4. Plot of the signal power as a function of frequency is shown for the return signal at a range of 23 m shown in Fig. 3. This plot was generated using a discrete Fourier transform that shows a modulated return signal near 220 Hz. The modulated return signal is generated by the wing-beat modulation of the scattered light, indicating the presence of a honeybee.

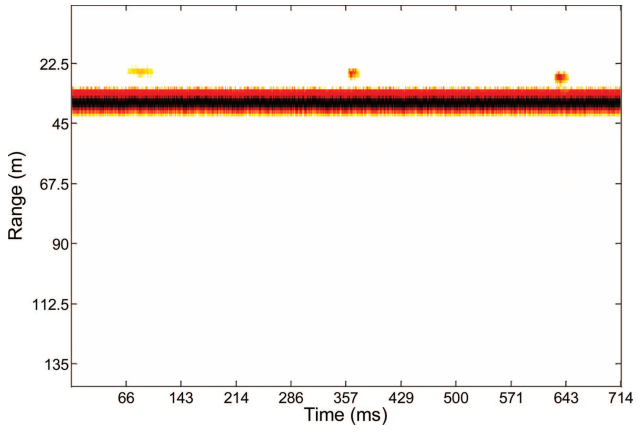

Fig. 6. (Color online) False-color image represents the strength of the return signal from a particular range as a function of time. In this figure, a strong return signal was seen at 35 m, while three shorter return signals were seen at ranges of 23, 25, and 30 m.

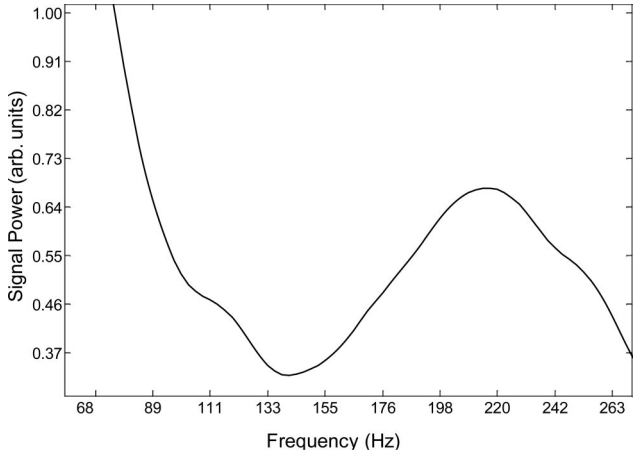

Fig. 7. Plot of the signal power as a function of frequency is shown for the return signal at a range of 25 m shown in Fig. 3. This plot was generated using a discrete Fourier transform. It shows a modulated return signal near 220 Hz. The modulated return signal is generated by the wing-beat modulation of the scattered light and indicates the scattering object was a honeybee. Similar results were found for the scattered light at ranges of 23 and 30 m.

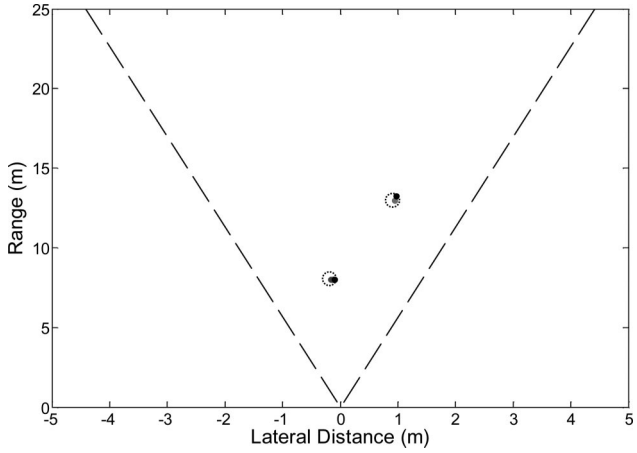

Fig. 9. Plot of the honeybee density as a function of location. The feeders are shown as the dashed circles, while the solid dots represent honeybee density measurements. The area between the two dashed lines indicates the area scanned by the instrument. Good agreement between the measured honeybee density with the expected honeybee density due to the feeders is seen in this figure.

mation for determining the detected honeybee behavior.

Initial testing of the ability of the instrument to detect and map honeybee density in a scanning mode was performed at the Montana State University beehive. Honeybees were chummed to two feeders filled with a sugar-water solution, producing a localized honeybee presence above the feeders. The lidar instrument was scanned above the feeders through a total angle of 20° with a step size of 0.4°, producing 50 unique angle bins. The lidar beam was scanned above the feeders a total of three times. These data were collected and processed using the software described in Section 2. In this case, each time an FFT detected spectral power above a threshold value in the frequency range of 200–300 Hz, a honeybee was assumed to be detected and the range and angle of the honeybee detection was recorded. This was completed for all three scans, and a spatial map indicating the honeybee densities was generated and is shown in Fig. 9. The solid circles indicate the areas of high honeybee density measured using the instrument described above, while the dotted circles indicate the location of the feeders used to create an increased local density of honeybees. The area between the two dashed lines indicates the area over which the instrument was scanned. Good agreement is seen between the feeder location and the higher honeybee density, indicating that this direct detection lidar instrument is capable of mapping honeybee densities.

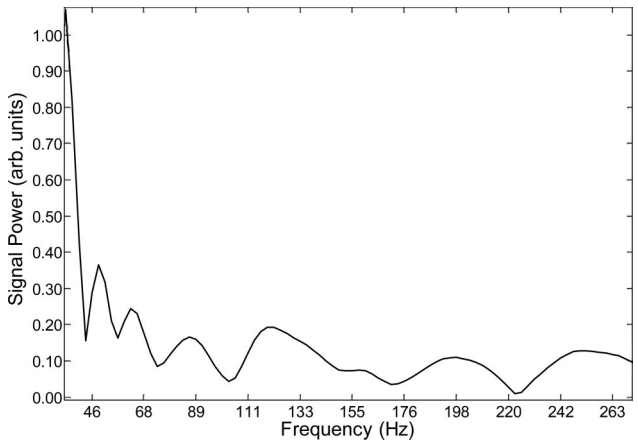

Fig. 8. Plot of the signal power as a function of frequency is shown for the return signal at a range of 36 m shown in Fig. 6. This plot was generated using a discrete Fourier transform and shows an unmodulated return signal, indicating that light was scattered from a stationary object. In this case, the scattering object was observed to be vegetation.

4. Conclusions

UXOs kill thousands of people each year, as well as make large areas of land unavailable for agriculture in some of the world's poorest countries. Efforts to speed up UXO removal is under investigation along many tracks of inquiry, including biological detection. One exciting avenue of research for UXO removal is to condition honeybees to use their natural foraging behavior to detect the vapor plume associated with the UXOs.[3–6] The honeybees can then be mapped using a lidar instrument to infer where the UXOs are located.[8] However, it was noted that a direct detection lidar was needed that was able to distinguish the return signal from honeybees and the return signal from other sources, such as vegetation. In this paper, a design of a novel, to the best of our knowledge, direct detection imaging lidar was presented that can be used to discern scattered light from honeybees with other sources including vegetation, by looking at the frequency content of the return signal through the use of discrete time FFTs. With appropriate software to analyze the two-dimensional

data arrays generated by this instrument, spatial maps of honeybee densities can then be produced.

This investigation was supported by the Alion Science and Technology Corporation through an award from the U.S. Army NightVision and ESD (DAAB07-03-D-203-006) to The University of Montana.

References

1. J. MacDonald, J. R. Lockwood, J. McFee, T. Altshuler, T. Broach, L. Carin, R. Harmon, C. Rapaport, W. Scott, and R. Weaver, *Alternatives for Landmine Detection* (RAND Corp., 2003), available at www.rand.org/publications/MR/MR1608/MR1608.appg.pdf.
2. J. M. Phelan and J. L. Barnett, "Chemical sensing thresholds for mine detection dogs," in Proc. SPIE **4742,** 532–543 (2002).
3. G. C. Smith, J. J. Bromenshenck, D. C. Jones, and G. H. Alnasseer, "Volatile and semivolatile organic compounds in beehive atmospheres," in *Honey Bees: Estimating the Environmental Impact of Chemicals,* J. Devillars and M.-H. Pham-Delegue, eds. (Taylor and Francis, 2002), Chap. 2, pp. 12–41.
4. J. J. Bromenshenk, C. B. Hendersen, and G. C. Smith, *Biological Systems: Alternatives for Landmine Detection,* RAND Science and Technology Institute for Office of Sciences and Technology Policy Report, J. MacDonald, J. R. Lockwood, J. McFee, T. Altshuler, T. Broach, L. Carin, C. Rappaport, W. R. Scott, and R. Weaver, eds. (RAND Corp., 2003), available at http://www.rand.org/publications/MR/MR1608.
5. J. J. Bromenshenk, C. B. Henderson, R. A. Seccomb, R. T. Etter, S. F. Bender, P. J. Rodacy, J. A. Shaw, N. L. Seldomridge, and L. H. Spangler, "Can honey bees assist in area reduction and landmine detection?" J. Mine Action **7.3,** (2003), available at http://www.maic.jmu.edu/journal/7.3/focus/bromenshenk/bromenshenk.htm.
6. J. J. Bromenshenk, C. B. Henderson, R. A. Succomb, L. H. Spangler, J. H. Shaw, K. S. Repasky, J. L. Carlesten, T. Balch, P. Rodacy, and S. Bender, *Technical Report-Study/Services, CRDL DI-MISC-80598A, for U.S. Joint Chiefs of Staff* (U.S. Department of Defense, 2004).
7. S. F. A. Bender, P. J. Rodacy, R. L. Smith, P. J. Hargis, Jr., M. S. Johnson, J. R. Klarkowsky, G. I. Magee, and G. L. Bender, *Tracking Honey Bees Using LIDAR (Light Detection and Ranging)* (Sandia National Laboratories Rep. SAND2003-0184, 2003).
8. J. A. Shaw, N. Seldomridge, D. L. Dunkle, P. W. Nugent, L. Spangler, J. J. Bromenshenk, C. B. Henderson, J. H. Churnside, and J. J. Wilson, "Polarization measurements of honeybees in flight for locating landmines," Opt. Express **13,** 5853–5863 (2005).
9. S. C. Reed, C. M. Williams, and L. E. Chadwick, "Frequency of wing-beat as a character for separating species races and geographic varieties of drosphila," Genetics **27,** 349–361 (1942).
10. D. M. Unwin and C. P. Ellington, "An optical tachometer for measurement of the wing-beat frequency of free-flying insects," J. Exp. Biol. **82,** 377–378 (1979).
11. A. Moore and R. H. Miller, "Automated identification of optically sensed aphid (homoptera: Aphidae) wing beat forms," Ann. Entomol. Soc. Am. **95,** 1–8 (2002).
12. K. S. Repasky, J. A. Shaw, R. Scheppele, C. Melton, J. L. Carlsten, and L. H. Spangler, "Optical detection of honeybees by use of wing-beat modulation of scattered laser light for locating explosives and land mines," Appl. Opt. **45,** 1839–1843 (2006).
13. A. V. Oppenheim, A. S. Willsky, and S. H. Nawab, *Signals and Systems,* 2nd ed. (Prentice Hall, 1997), pp. 514–581.